Original Article - Urological Oncology

Investig Clin Urol 2021;62:423-429.
https://doi.org/10.4111/icu.20200605
pISSN 2466-0493 • eISSN 2466-054X

INVESTIGATIVE AND CLINICAL UROLOGY
ICUROLOGY

Possible clinical implications of prostate capsule thickness and glandular epithelial cell density in benign prostate hyperplasia

Katherine G. Holder[1], Bernardo Galvan[1], Andrew S. Knight[1], Freedom Ha[1], Reagan Collins[1], Preston E. Weaver[1], Luis Brandi[2], Werner T. de Riese[1]

Departments of [1]Urology and [2]Pathology, Texas Tech University Health Sciences Center, Lubbock, TX, USA

Purpose: The negative correlation between BPH-size and incidence of prostate cancer (PCa) is well-documented in the literature, however the exact mechanism is not well-understood. The present study uses histo-anatomical imaging to study prostate volume in correlation to prostate capsule thickness, and glandular epithelial cell density within the peripheral zone (PZ).

Materials and Methods: Specimens were selected from radical prostatectomies ranging from 20 to 160 mL based on ease of anatomical reconstruction by the slides. A total of 60 patients were selected and underwent quantitative measurements of prostate capsule thickness and glandular epithelial density within the PZ using computer-based imaging software. Pearson's correlation and a stepwise multiple linear regression analysis was conducted to determine the relationship between these measured parameters and the clinical characteristic of these patients.

Results: Pearson's correlation analysis revealed a strongly significant, negative correlation between prostate volume and glandular epithelial cell density ($r(58)=-0.554$, $p<0.001$), and a strongly significant, positive correlation between prostate volume and average capsule thickness ($r(58)=0.462$, $p<0.001$). Results of multiple regression analysis showed that average glandular epithelial cell density added statistically to this prediction ($p<0.05$).

Conclusions: The results suggest that growth of the transition zone in BPH causes increased fibrosis of the PZ, leading to atrophy and fibrosis of glandular cells. As 80% of PCa originates from the glandular epithelium within the PZ, this observed phenomenon may explain the inverse correlation between BPH and PCa that is well-documented in the literature.

Keywords: Image processing; Prostate; Prostatic hyperplasia

INTRODUCTION

Prostate cancer (PCa) and benign prostate hyperplasia (BPH) are the two most common urological disorders affecting older males, with PCa being amongst the most common types of cancers affecting males, and with more than half of the male population over the age of 50 years showing either clinical and/or histological evidence of BPH [1]. Both PCa and BPH are characterized by proliferation of prostatic tissue. In the United States, PCa accounts for 20% of all new cancer diagnoses and has been the leading cause of new cancer cases in males in recent years. Second only to lung

Received: 3 January, 2021 • **Revised:** 23 February, 2021 • **Accepted:** 1 March, 2021 • **Published online:** 31 May, 2021
Corresponding Author: Werner T. de Riese https://orcid.org/0000-0003-1963-2334
Department of Urology, Texas Tech University Health Sciences Center, 3601 4th Street, MS7260, Lubbock, TX 79430-7260, USA
TEL: +1-806-743-3862, FAX: +1-806-743-3030, E-mail: werner.deriese@ttuhsc.edu

cancer in cancer related deaths, PCa kills more than 33,300 males each year, and males have a 12% chance of developing invasive PCa throughout their lifetime [2]. While there has been correlations shown between the presence of BPH and PCa, recent studies have shown an inverse correlation in the size of the prostate in relation to clinically significant cancer. Review of the literature has revealed very few studies attempting to explain the mechanism through which BPH may inhibit the development of PCa [1,3]. Previous studies have shown that larger prostates are associated with increased capsule thickness and greater extent of glandular atrophy within the peripheral zone (PZ), suggesting an expansion of the transition zone (TZ) of the prostate against its capsule causing secondary compression-induced atrophy and fibrosis of glandular tissue within the PZ [4,5].

Limited studies have been reported about BPH-related histomorphological changes of prostatic glands. One preliminary pilot study has been completed in which prostate size was compared to prostate capsule thickness and prostate glandular density in small and large prostates [6]. Based on this preliminary study, we have analyzed the histomorphological features in prostates of all sizes, utilizing a similar pixel imaging technique described in the previous paper, allowing for isolation of glandular epithelium and measurement of glandular epithelial volume alone.

MATERIALS AND METHODS

In order to examine the relationship between histological changes within the PZ and BPH, a retrospective study was conducted comparing the overall volume of the prostate with the following two parameters: (1) glandular epithelial cell density within the PZ next to the capsule; and (2) thickness of the peripheral fibrotic layer (also called the 'surgical capsule' or 'capsule').

After approved by the Institutional Review Board of the Texas Tech University Health Sciences Center, Lubbock, Texas, USA (approval number: L20-128). Informed consent was waived by the board. Sixty patients were selected who had undergone radical prostatectomy between 2010 and 2020. Patient selection was based on ease of reconstruction of the prostate anatomy by the anatomical slides to identify the exact location of measurements. Grossing techniques vary greatly among pathologists, with some using sagittal or transverse cuts, while others use coronal cuts, leading to differences in the orientation of the prostate within anatomical slides. In order to obtain reproducible measurements from corresponding areas of the prostate, patients were selected from a group of two pathologists who consistently utilized transverse dissection of prostate specimens and who provided clear anatomical diagrams of the locations of those cuts within the prostate. Specimens were taken from prostates of all sizes, with prostate volume ranging from 20 mL to 160 mL. A total of 60 patients were selected for the quantitative measurements. None of these patients had undergone any previous ablative (such as transurethral resection of the prostate including laser or partial prostatectomy) or medical (such as androgen deprivation therapy or alpha-blockers) treatment. Previous studies have shown that the PZ is mainly present in the dorsal aspect of the prostate, it is less pronounced at the lateral aspects, and it phases out towards the anterior aspect, base, and apex. Due to these anatomical findings, slides of interest were chosen that represented the two most equatorial slices (on the dorsal aspect, halfway between the base and the apex of the prostate, see also Fig. 1). Not all prostate specimens and slices were usable due to extension of PCa into areas of interest or due to inability to reconstruct the anatomy of the prostate. Two equatorial slices were measured at the 4:00, 6:00, and 8:00 positions of the posterior portion of the prostate, resulting in 6 measurements per prostate specimen. Measurements from the inferior and superior portions of the equatorial region allowed development of a representative three-dimensional structure analysis of prostatic tissue regarding prostatic glandular epithelial tissue and the prostate capsule within the PZ.

Once selected, the H&E slides of each prostate were

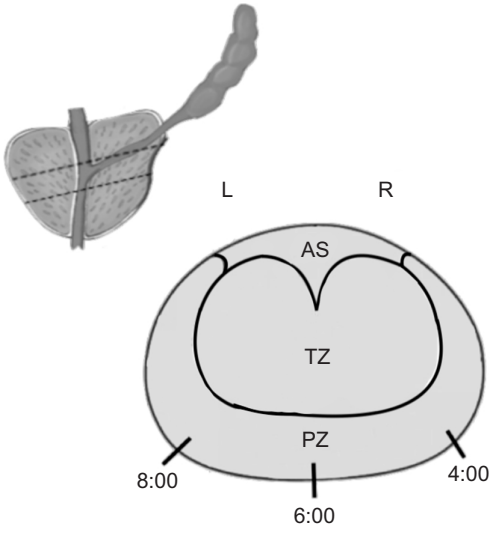

Fig. 1. Anatomical diagram of the prostate. A transverse section extending from anterior to posterior prostate, through the mid-gland, across the urethra, within the equatorial zone of the prostate, showing the different zones of the prostate–the anterior stroma (AS), transition zone (TZ), and peripheral zone (PZ). Measurements were taken at the 4:00, 6:00, and 8:00 regions, above and below the equatorial zone, as shown in the upper left-hand corner. L, left; R, right.

https://doi.org/10.4111/icu.20200605

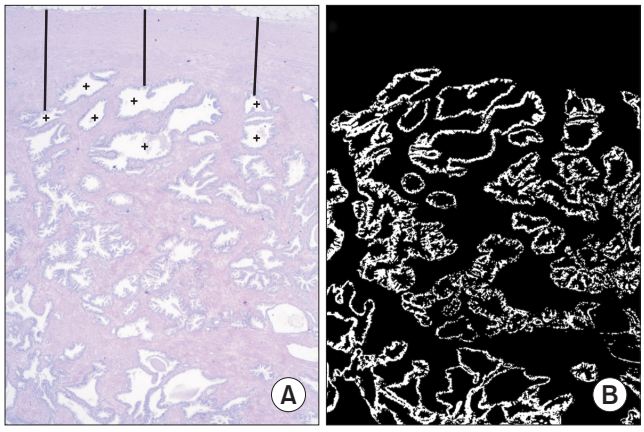

Fig. 2. Example of a small prostate (31 mL) for image processing. Thick lines indicate measurements for average capsule thickness. Normal glands are indicated by "+" symbol. (A) Showing H&E stain at 50× magnification. (B) Glandular pixel visualization of the same prostate specimen after pixel intensity processing, excluding surrounding connective tissue and non-glandular structure in the peripheral zone.

examined using light microscopy (LEICA DM 100; LEICA, Wetzlar, Germany) via 5× objective lens. Images were acquired using a LEICA MC170 HD camera (LEICA) and its associated LEICA Application Suite software (LEICA). Image acquisition was standardized by juxtaposing the outer boundary of the prostate capsule along the edge of the image as close as possible. Initial processing was completed within LEICA Application Suite (LEICA), allowing image sharpening and adjustment of contrast prior to the image being saved to our files. Further processing was achieved using ImageJ (National Institutes of Health, Bethesda, MD, USA), a Java-based open-source image processing software [7]. Measurement calibration was achieved using the image of a transparent ruler under the same magnification specifications described previously. A linear measurement of 1 mm of ruler allowed the software to determine the number of pixels contained within 1 mm of imaging. With this calibration, prostate capsule thickness was calculated using the average of three linear measurements from the outer edge to the inner edge of the prostate capsule, where there was absence of glandular atrophy and surrounding fibrosis. Glands within the capsule appeared atrophic.

The Color Deconvolution plugin, a freely available add-on to ImageJ, was applied to images taken from the PZ. The Color Deconvolution plugin uses a method described by Ruifrok and Johnston [8] to separate individual dyes in stained specimens. We used the included H&E 3,3′-Diaminobenzidine vector to isolate glandular epithelial tissue from surrounding stroma. Further contrast processing was applied to increase the color differences between glandular epithelial tissue and surrounding stroma. Nerves, blood vessels, empty space outside the capsule, and other artifacts were manually cropped out of our image. The image was then converted to grayscale and a threshold was applied to eliminate pixels under a certain color intensity value cutoff, allowing removal of surrounding stroma and leaving only pixels representing glandular epithelial tissue behind (Fig. 2B). The measuring tool was then used to determine the surface area percentage occupied by glandular epithelial tissue alone, giving us an accurate and quantitative estimation of glandular epithelial volume for the tissue sample.

Statistical analysis

Descriptive statistics were performed and are summarized in Table 1 as mean±standard deviation, median (interquartile range) for continuous variables, and as frequency (percentage) for categorical variables. Average glandular epithelial cell density and average capsule thickness were calculated using the six measurements. Pearson's correlation was conducted to assess the correlation between prostate volume with average capsule thickness and glandular epithelial density. A stepwise multiple linear regression analysis was conducted to build a prediction model after testing for assumptions of linearity, heteroscedasticity, independence, outliers, multicollinearity, and residuals. A significance level of $p<0.05$ was set as statistically significant. All the statistical analyses were performed using SPSS version 26 (IBM Corp., Armonk, NY, USA).

RESULTS

Prostate volume ranged from 20 mL to 160 mL, with a mean of 55.53 mL and a standard deviation of 33.27 mL. Average epithelial cell density ranged from 0.01 to 0.24, with a mean of 0.09 and a standard deviation of 0.05. Average prostate capsule thickness ranged from 1.42 mm to 10.88 mm, with a mean of 6.78 mm and a standard deviation of 2.82 mm. Results from Pearson's correlation analysis suggest that there is a strongly significant, negative correlation between prostate volume and glandular epithelial cell density, ($r(58)=-0.554$, $p<0.001$) and a strongly significant, positive correlation between prostate volume and average capsule thickness ($r(58)=0.462$, $p<0.001$). The multiple regression model tested the association between prostate volume with the following independent variables: age, race, height, weight, Charlson Comorbidity Index, ASA (American Society of Anesthesiologists) Physical Status Classification System, smoker, prostate specific antigen (PSA), PSA density, Gleason Score of final pathology reading, pathologic stage, tumor volume, average capsule thickness, and average glandular epithelial cell

Table 1. Patient demographics and characteristics

Variable	n (%)	Mean±SD	Median (IQR)	Minimum	Maximum
Age (y)		63.5±7.68	64 (58.25–69.75)	35	75
Height (cm)		176.8±7.47	178.05 (172.72–182.88)	160.02	191.01
Weight (kg)		91.77±17.76	92.08 (77.86–101.60)	63.37	151.95
Charlson Comorbidity Index		4.55±1.41	4 (3–5)	2	9
ASA Physical Status Classification System		2.5±0.54	2 (2–3)	2	4
PSA (ng/mL)		10.11±9.94	7.3 (5.16–10.82)	1.4	68.39
PSA density		0.27±0.26	0.19 (0.11–0.34)	0.02	1.72
Gleason Score of final pathology reading[a]		6.88±0.46	7 (7–7)	6	8
Prostate volume (mL)		55.53±33.27	20 (31.25–71.5)	20	160
Tumor volume (mL)		7.12±5.67	5.26 (3.05–9.15)	0.81	30
Average glandular epithelial cell density		0.09±0.05	0.09 (0.05–0.12)	0.01	0.24
Average capsule width (mm)		6.78±2.82	7.30 (4.47–9.26)	1.42	10.88
Race					
White	43 (71.7)				
Black	7 (11.7)				
Hispanic	10 (16.6)				
Smoker					
Non-smoker	30 (50.0)				
Prior smoker	18 (30.0)				
Current smoker	12 (20.0)				
Surgical approach					
Open	22 (36.7)				
Laparoscopic	36 (60.0)				
Robotic	2 (3.3)				
Pathologic stage					
No cancer found in final prostatectomy specimen	1 (1.7)				
pT2	44 (73.3)				
pT3	15 (25.0)				
Pathologic nodal stage					
NX	15 (25.0)				
N0	43 (71.7)				
N1	2 (3.3)				

SD, standard deviation; IQR, interquartile range; ASA, American Society of Anesthesiologists; PSA, prostate specific antigen.
[a]:Case with no cancer in final specimen was excluded.

Table 2. Summary of multiple linear regression

Parameter	B	SE_b	p-value	95% CI lower	95% CI upper
(Constant)	68.39	18.48	<0.001	31.38	105.40
Average capsule width	2.25	1.64	0.175	-1.03	5.53
Average glandular epithelial cell density	-3.11	0.99	0.003	-5.10	-1.12

B, unstandardized regression coefficient; SE_b, standard error of the coefficient; CI, confidence interval.

density. In our study, the multiple regression model statistically significantly predicted prostate volume. Out of all the variables in the model, only average glandular epithelial cell density added statistically to the prediction ($p<0.05$), concluding that for every 1% increase in average glandular epithelial cell density, the prostate volume decreases by 3.11 mL. Regression coefficients and standard errors can be found in Table 2. Based on the adjusted R2, average glandular epithelial cell density explained 30.7% of the variability in prostate volume (Fig. 3).

DISCUSSION

Understanding the intricacies of prostate anatomy is es-

https://doi.org/10.4111/icu.20200605

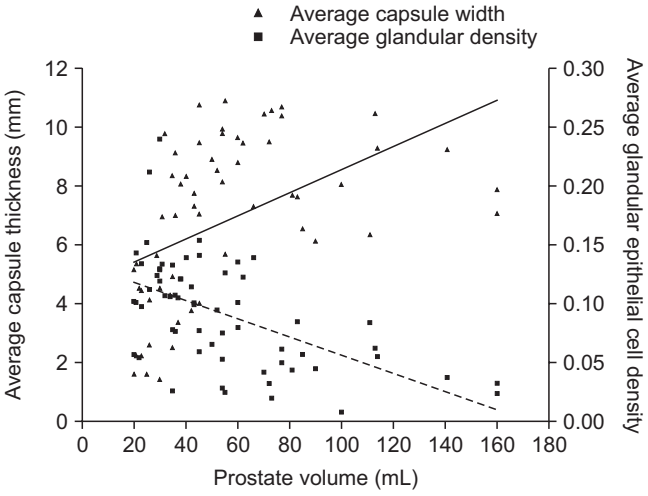

Fig. 3. Average capsule width and average glandular epithelial cell density plotted against prostate volume with linear predictors and 95% confidence interval.

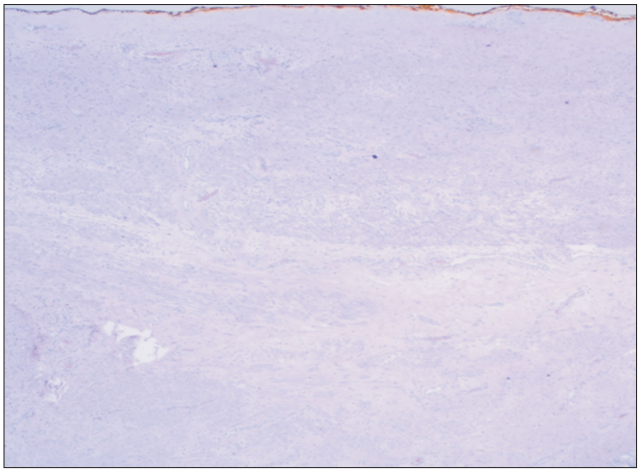

Fig. 4. Example of a large prostate (113 mL), showing atrophy and fibrosis as well as a thick capsule covering the entire H&E image (12 mm) at 50× magnification. This image reveals severe gland atrophy when compared to a smaller prostate as seen in Fig. 2A.

sential for analyzing the physiologic interactions between BPH and PCa. Anatomically, the prostate can be divided into an inner TZ, an anterior stroma (AS), and an outer PZ surrounded by a capsule as illustrated in Fig. 1 [4]. There is a small central zone surrounding the ejaculatory ducts near the base of the prostate. The majority of the prostate's glandular tissue is found in the PZ [4]. In young adult males, the prostatic capsule is a dense fibromuscular tissue composed of an inner smooth muscle layer and an outer collagenous membrane [4]. The literature unanimously agrees that BPH growth originates in the prostate's TZ which increases in length and volume during the disease process [9]. In contrast, PCa arises from glandular tissue of the PZ in up to 85% of cases [10]. The anatomical location of these disease processes may be key in understanding the pathophysiology underlying the relationship/interaction between BPH and PCa.

There is overwhelming evidence in the literature for an inverse relationship between BPH size and PCa incidence [10]. Patients with large BPH prostates experience lower incidence of PCa and less severe PCa disease than patients with smaller prostates [11]. The mechanism of this relationship is still not well understood, and new research techniques have focused on this in recent years. Ultrasound, magnetic resonance imaging, and mathematical models have all been applied to investigate structural changes in prostate anatomy that underlie BPH and PCa [12–14].

It is well documented in the literature that prostate volume inversely correlates with incidence and severity of PCa [10]. Furthermore, numerous studies have proven that the majority of growth in BPH originates in the TZ [15]. However, prostatic hyperplasia is limited by the fibrous prostatic capsule which resists growth from the TZ [14]. The opposing forces of TZ growth and capsular constraints cause increasing pressure on the glandular tissue of the PZ. This compression-induced force ultimately transforms the architecture of the PZ's glandular tissue into atrophic fibrosis contributing to a thickening prostatic capsule in large BPH prostates (an example is demonstrated in Fig. 4) [4].

The anatomical capsule in young males is a 'false capsule' that forms posteriorly and laterally around the prostate (and is mainly absent in the anterior aspect of the prostate). This anatomical capsule derives from the periprostatic pelvic fascia and is composed of smooth muscle cell layers with an outer collagenous layer [16]. As outlined in our study, large BPH prostates develop a fibrotic and collagenous layer inwardly from the anatomical capsule, giving the appearance of thickening of the anatomical capsule. Since the introduction of BPH surgery, experienced urologists call this thickened fibrotic layer in large BPH the 'surgical capsule', a well-known phenomenon in large BPH prostates (>80 mL, where the surgical capsule allows the surgeon an easy enucleation of the BPH component/removal of the adenoma) [17]. This surgical phenomenon is much less pronounced and smaller prostates.

As the TZ grows, it compresses cells within the PZ causing changes in tissue organization and development of fibrotic layers adjacent to the anatomical capsule.

The results of our study showed that expansion of the TZ seen in BPH causes histo-anatomical changes within the PZ. The decreased glandular density and increased capsular thickness seen in larger prostates suggest that growth of the TZ causes widespread atrophy and apoptosis of the PZ

glands along with fibrosis of tissue surrounding the glands. This widespread fibrosis and collagen deposition within PZ tissues represent the thickened surgical capsule seen in larger prostate specimens. The histo-anatomical changes in tissue architecture with widespread atrophy and apoptosis of the PZ glandular epithelium seen in large BPH prostates may be one of the main mechanisms causing the reduced PCa incidence described in many clinical studies.

In a previous pilot study, 20 prostates that fell into a small (<30 mL) or large (>70 mL) category were measured and analyzed, which found that prostate volume correlated directly with capsule thickness and inversely with glandular tissue density. In this follow-up study, we selected 60 prostates ranging from 20 mL to 160 mL with no size exclusions. Even with the diversity in volume, the data upheld the previous results: epithelial cell density decreased and capsule thickness increased with prostate volume. To our knowledge, this study analyzing prostate specimen with pixel imaging technology is the largest of its kind, and it further supports the previous findings in providing a potential mechanism by which BPH may be protective against PCa.

Although sample size has increased significantly from the previous pilot study, we are still aware of some study limitations. Reconstructing prostatic anatomy from dozens of slides proved challenging. Additionally, slides that were affected by PCa had to be excluded as cancerous tissue disrupted the normal PZ and capsular architecture. Additionally, capsule thickness varies significantly within each prostate and in some cases, the boundary between prostate capsule and BPH tissue can be difficult to identify.

Despite these limitations, this study provides further evidence in supporting the hypothesis that BPH may be protective against PCa. We hope our study encourages other clinicians and researchers to further investigate the relationship between PCa and BPH. If the hypothesis of protective features within BPH against PCa is correct, it will impact future diagnosis and treatment of BPH and PCa.

CONCLUSIONS

This study outlines a possible mechanism of the histo-anatomical changes explaining the well-documented inverse correlation between BPH and PCa. The TZ enlargement in BPH patients compresses the PZ against the prostate's anatomical capsule and causes the capsule to thicken while simultaneously inducing glandular atrophy and fibrosis within the PZ. This mechanism, in large BPH prostates, may be protective against PCa. Our study should encourage further investigation into the relationship between prostate volume and the incidence and severity of PCa. If the hypothesis is correct, there will be relevant clinical implications on the future diagnosis and treatment of BPH and PCa.

CONFLICTS OF INTEREST

The authors have nothing to disclose.

ACKNOWLEDGMENTS

All contributions provided by authors or coauthors.

AUTHORS' CONTRIBUTIONS

Research conception and design: Werner T. de Riese. Data acquisition: Andrew S. Knight, Bernardo Galvan, Katherine G. Holder, and Freedom Ha. Data analysis and interpretation: Reagan Collins. Drafting of the manuscript: Preston E. Weaver and Katherine G. Holder. Supervision: Werner T. de Riese, Preston E. Weaver, and Luis Brandi. Approval of the final manuscript: Werner T. de Riese.

REFERENCES

1. Alcaraz A, Hammerer P, Tubaro A, Schröder FH, Castro R. Is there evidence of a relationship between benign prostatic hyperplasia and prostate cancer? Findings of a literature review. Eur Urol 2009;55:864-73.
2. American Cancer Society. Cancer facts & figures 2020 [Internet]. Atlanta (GA): American Cancer Society; 2020 [cited 2020 Jan 24]. Available from: https://www.cancer.org/content/dam/cancer-org/research/cancer-facts-and-statistics/annual-cancer-facts-and-figures/2020/cancer-facts-and-figures-2020.pdf.
3. de Gorski A, Rouprêt M, Peyronnet B, Le Cossec C, Granger B, Comperat E, et al. Accuracy of magnetic resonance imaging/ultrasound fusion targeted biopsies to diagnose clinically significant prostate cancer in enlarged compared to smaller prostates. J Urol 2015;194:669-73.
4. Fine SW, Reuter VE. Anatomy of the prostate revisited: implications for prostate biopsy and zonal origins of prostate cancer. Histopathology 2012;60:142-52.
5. Strasser H, Janetschek G, Reissigl A, Bartsch G. Prostate zones in three-dimensional transrectal ultrasound. Urology 1996;47:485-90.
6. Weaver PE, Smith LA, Sharma P, Keesari R, Al Mekdash H, de Riese WT. Quantitative measurements of prostate capsule and gland density and their correlation to prostate size: possible clinical implications in prostate cancer. Int Urol Nephrol 2020;52:1829-37.

https://doi.org/10.4111/icu.20200605

7. Collins TJ. ImageJ for microscopy. Biotechniques 2007;43(1 Suppl):25-30.
8. Ruifrok AC, Johnston DA. Quantification of histochemical staining by color deconvolution. Anal Quant Cytol Histol 2001;23:291-9.
9. Zhang SJ, Qian HN, Zhao Y, Sun K, Wang HQ, Liang GQ, et al. Relationship between age and prostate size. Asian J Androl 2013;15:116-20.
10. Peng Y, Shen D, Liao S, Turkbey B, Rais-Bahrami S, Wood B, et al. MRI-based prostate volume-adjusted prostate-specific antigen in the diagnosis of prostate cancer. J Magn Reson Imaging 2015;42:1733-9.
11. Moschini M, Gandaglia G, Suardi N, Fossati N, Cucchiara V, Damiano R, et al. Importance of prostate volume in the stratification of patients with intermediate-risk prostate cancer. Int J Urol 2015;22:555-61.
12. Al-Khalil S, Ibilibor C, Cammack JT, de Riese W. Association of prostate volume with incidence and aggressiveness of prostate cancer. Res Rep Urol 2016;8:201-5.
13. Chang E, Jones TA, Natarajan S, Sharma D, Simopoulos D, Margolis DJ, et al. Value of tracking biopsy in men undergoing active surveillance of prostate cancer. J Urol 2018;199:98-105.
14. Lorenzo G, Hughes TJR, Dominguez-Frojan P, Reali A, Gomez H. Computer simulations suggest that prostate enlargement due to benign prostatic hyperplasia mechanically impedes prostate cancer growth. Proc Natl Acad Sci U S A 2019;116:1152-61.
15. Holder K, Galvan B, Sakya J, Frost J, de Riese W. Anatomical changes of the peripheral zone depending on benign prostatic hyperplasia size and their potential clinical implications: a review for clinicians. Urol Pract 2021;8:259-63.
16. Ayala AG, Ro JY, Babaian R, Troncoso P, Grignon DJ. The prostatic capsule: does it exist? Its importance in the staging and treatment of prostatic carcinoma. Am J Surg Pathol 1989;13:21-7.
17. Semple JE. Surgical capsule of the benign enlargement of the prostate. Its development and action. Br Med J 1963;1:1640-3.